Interaction of exciton polaritons with the surface potential of thin semiconductor films: *s*-polarization geometry

B. Flores-Desirena, F. Pérez-Rodríguez, and P. Halevi
Instituto de Física de la Universidad Autónoma de Puebla, Apartado Postal J-48, Puebla, Puebla 72570, México
(Received 23 March 1994)

The influence of the surface-potential shape on exciton optical spectra for thin semiconductor films is investigated theoretically. Using a realistic model with both intrinsic and extrinsic contributions, we calculate the polarization vector and the electric field in the case of *s*-polarized incident light at one of the thin-film surfaces. Our analytic results are employed to study the relation between the surface potential parameters and the spectra of reflectivity and transmissivity. The generation of near-surface localized excitons and their optical manifestation are also analyzed.

I. INTRODUCTION

It is well known that the optical properties of excitonic semiconductors depend notably on the nature of the exciton confinement.[1] That is, the optical spectra of confined systems are determined by the characteristics of the exciton motion. Among confined systems, the thin semiconductor film is an interesting example. If one considers only undistorted excitons, then the thin film must have a thickness substantially larger than the exciton radius. Therefore, the spatial confinement in thin films produces the quantization of the exciton wave vector, corresponding to its translational motion.[2] This exciton quantization gives rise to resonances in the spectra of reflectivity and transmission. The interaction of excitons with the sample surfaces affects the shape and the position of these spectral resonances.

In the case of thin intrinsic-semiconductor films, the effect of the near-surface transition layers[3] on the optical spectra has been studied intensively (see, for example, Refs. 4–8 and 10–20). In some works,[4,6–8] the simple model of the "dead layer" (or "exciton-free layer") (Ref. 9) was utilized to calculate the transmission and reflection coefficients of thin, spatially dispersive, films. It was shown that spectra of thin films can be explained by a multimode polariton interference, which is strongly affected by the presence of dead layers and by the additional boundary conditions (ABC) employed. These results allowed the authors to describe some important features of spectra observed in experiments.[10–13] Recently[14–20] a more sophisticated approach to the exciton-surface interaction was applied in thin films. Within this approach, the distortion of the exciton wave function due to the film surfaces is taken into account through evanescent components which exponentially vanish over distances of the order of the transition-layer thickness. It is noteworthy that Refs. 18 and 2 demonstrate the relationship between the size quantization of the exciton's translational motion and the multimode polariton interference.

Transition layers at surfaces can also be described by continuous surface potentials.[3] Thus it is possible to investigate not only intrinsic (repulsive) transition layers, but also layers with an extrinsic contribution.[21] Surface treatments such as doping, illumination, electron and ion bombardment, etc., produce impurity ions in the sample. Consequently, a near-surface space-charge region is formed, giving an extrinsic contribution to the surface potential, which may become attractive. The optical manifestation of localized excitons within a surface-potential well has been widely studied for semi-infinite systems (see Refs. 21–23 and references therein). In the case of thin films with a surface-potential well, calculations of reflectance and transmission have been carried out only with the aid of a multistep model for the potential,[24] and with an effective boundary condition replacing the potential.[25]

The aim of the present work is to investigate the motion of excitons in a thin semiconductor film with a realistic, continuous surface potential. We shall analyze the dependence of the spectra of reflectivity and transmissivity on the parameters characterizing the potential. In the analysis, both intrinsic and extrinsic surface potentials are considered. Special attention is paid to the generation of bound exciton states within the potential well. This work represents a logical extension of Ref. 21, which was devoted to a semiconductor surface.

In Sec. II we solve analytically the system of equations describing the propagation of exciton polaritons in thin semiconductor films, with the surface potential modeled as a truncated Morse potential.[21] The results of calculating the reflectivity and transmissivity for different intrinsic-semiconductor films are presented in Sec. III. Finally, in Sec. IV we study the effect of extrinsic surface potential wells on the optical spectra.

II. THEORY

Let us consider a thin semiconductor film with surfaces at planes $z=0$ and L. The spaces $z<0$ and $z>L$ are occupied by a vacuum. Assuming that *s*-polarized light is incident at the surface $z=0$, the electric field in the vacu-

um can be expressed in the form

$$\mathbf{E}(x,z,t)=(0,E(x,z,t),0) ,$$
$$E(x,z,t)=\begin{cases}(E_i e^{iq_z z}+E_r e^{-iq_z z})e^{iq_x x-i\omega t} , & z<0\\ E_t e^{i(q_x x+q_z z)-i\omega t} , & z>L ,\end{cases} \tag{1}$$

where

$$q_x=q\sin\theta,\quad q_z=q\cos\theta,\quad q=\omega/c . \tag{2}$$

θ is the angle of incidence, ω is the frequency, and c is the speed of light in vacuum. The quantities E_i, E_r and E_t in Eq. (1) denote the amplitudes of the incident, reflected, and transmitted fields, respectively.

Inside the semiconductor film ($0<z<L$) the electric field **E** is coupled to the excitonic polarization vector **P**. These fields are described by a system of two differential equations (see, for example, Refs. 3 and 21). One of the equations is derived from the exciton motion and the other is obtained from Maxwell's equations. For the *s*-polarization geometry, this system has a form as in Eq. (I.5) (hereafter I refers to our previous work, Ref. 21). Following this work, system (I.5) can be reduced to one equation for the y component of the excitonic polarization [i.e., for $P(z)$]:

$$\frac{\partial^4}{\partial z^4}P+\left[\varepsilon_0\frac{\omega^2}{c^2}-q_x^2+\Gamma^2(z)\right]\frac{\partial^2}{\partial z^2}P+2\frac{\partial\Gamma^2}{\partial z}\frac{\partial P}{\partial z}+\left[\left[\varepsilon_0\frac{\omega^2}{c^2}-q_x^2\right]\Gamma^2(z)-\frac{\omega_P^2\omega^2 M}{c^2\hbar\omega_T}+\frac{\partial^2\Gamma^2}{\partial z^2}\right]P=0 . \tag{3}$$

Here we have employed the same notation as in Ref. 21. The quantity $\Gamma^2(z)$ in Eq. (3) contains the surface potential $U(z)$ [see Eqs. (I.6) and (I.7)], for which we propose the model

$$U(z)=\begin{cases}U_1e^{-z/a}+U_2e^{-2z/a}+U_3e^{-(L-z)/b}+U_4e^{-2(L-z)/b} , & 0<z<L\\ \infty , & z=0 \text{ and } z=L .\end{cases} \tag{4}$$

The potential $U(z)$ (4) represents, in fact, a superposition of two generalized Morse surface potentials.[21] With this continuous model for $U(z)$, real surface potentials of semiconductor samples can be appropriately simulated. So, adjusting the parameters U_j ($j=1$, 2, 3, and 4), model (4) can describe intrinsic repulsive potentials for both surfaces [see Fig. 1(a)], or, also, extrinsic potential wells near treated surfaces [see Fig. 1(b)]. Furthermore, introducing imaginary parts in the parameters U_j ($j=1$, 2, 3, and 4), it is possible to take into account the variation of the damping [$\Delta\nu(z)=-2\,\mathrm{Im}U(z)/\hbar$] in the transition layers of the film.

In order to solve Eq. (3) with the assumed potential (4), we shall write $P(z)$ in the form

$$P(z)=\sum_{s=1}^{4}A_s e^{iq_s z}F_s(z) ,$$
$$F_s(z)=a_{0s}+\sum_{n=1}^{\infty}[a_{ns}e^{-nz/a}+b_{ns}e^{-n(L-z)/b}] , \tag{5}$$

where q_s ($s=1$, 2, 3, and 4) is the z component of the wave vectors corresponding to the plane waves which propagate in the bulk of the semiconductor film. The expressions for q_1 and q_2 are given by Eq. (I.12), while $q_3=-q_1$ and $q_4=-q_2$. The coefficients a_{ns} and b_{ns} in Eq. (5) should be found by using Eq. (3). Nevertheless, this can be accomplished only in the case when

$$e^{-L/a}\ll 1 \quad\text{and}\quad e^{-L/b}\ll 1 . \tag{6}$$

In the Appendix the coefficients a_{ns} and b_{ns} are calculated in the leading approximation in the parameters $\exp(-L/a)$ and $\exp(-L/b)$ (6). Consequently, our results are valid for films in which the interaction between surface layers can be neglected.

Employing expression (5) for $P(z)$ and the first equation in (I.5), we obtain the electric field $E(z)$ within the film ($0<z<L$) as follows:

$$E(z)=-\frac{4\pi\hbar\omega_T}{\omega_P^2 M}\sum_{s=1}^{4}A_s e^{iq_s z}\left[\frac{\partial^2 F_s(z)}{\partial z^2}+[\Gamma^2(z)-q_s^2]F_s(z)\right] . \tag{7}$$

The continuity conditions on the tangential components of the electric and magnetic fields at $z=0$ and L together with conditions $P(0)=0$ and $P(L)=0$, which

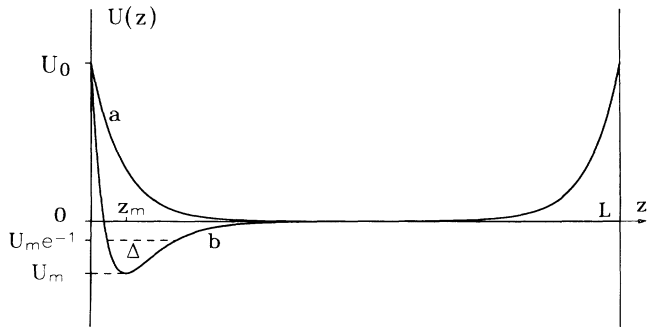

FIG. 1. Surface potentials in a thin semiconductor film: (a) intrinsic, (b) extrinsic, with a potential well.

are a consequence of the vanishing of the exciton wave function at the surfaces,[21] lead to a system of equations for the amplitudes E_r, E_t, and A_s ($s=1$, 2, 3, and 4). After solving this system, the reflectivity $R=|E_r/E_i|^2$ and transmissivity $T=|E_t/E_i|^2$ are calculated easily.

III. REPULSIVE TRANSITION LAYERS

First, we shall present the results obtained by computing the reflectivity and transmissivity for thin intrinsic-semiconductor films. In this kind of film the surface potential is symmetric with respect to its central plane, i.e., $U(z)=U(L-z)$. Moreover, the intrinsic transition layers are well described by repulsive exponential potentials.[3,21] We can choose the parameters of the model (4) for $U(z)$ as follows:

$$U_1=U_3=U_S\ ,\quad U_2=U_4=0\ ,\quad a=b\ , \tag{8}$$

where U_S is the height of the potential at both surfaces [$U_S\equiv U(0)=U(L)$]. Note that for this exponential model (8) the parameter a in Eq. (4) denotes the transition-layer thickness.

Figures 2 and 3 show the calculated spectra of normal-incidence ($\theta=0$) reflectivity and transmissivity for a CdS film ($L=1000$ Å). The parameters of the material used here are[26] $\varepsilon_0=9.1$, $M=0.94m$ (m is the free-electron mass), $\hbar\omega_T=2.55272$ eV [$A(n=1)$ is the exciton resonance], $\hbar\omega_P=0.29396$ eV and $\hbar\nu=0.124$ meV. From Fig. 2 it is evident that the increase of the effective transition-layer thickness a leads to a blueshift of the spectral resonances. This dependence of maxima and minima of optical spectra on the value of a was also demonstrated with the dead-layer[7,8] and microscopic[16,18] models. Notice that the shift of a resonance above the longitudinal frequency ω_L (at $\omega_i\geq\omega_L$), as a is increased, can be approximated by the same formula as for a thin film with dead layers of thickness a:[7]

$$\omega_i(a')-\omega_i(a)\approx 4[\omega_i(a)-\omega_T]\frac{a'-a}{L_{\text{eff}}}\ . \tag{9}$$

This result can be understood in terms of the quantization of the exciton translational motion in a film with effective thickness $L_{\text{eff}}=L-2a$.[16,18,19] Indeed, with increasing parameter a, the quantity L_{eff} decreases and the exciton eigenenergies grow. For this reason the spectral resonances, associated with these eigenenergies,[2] undergo a blueshift. We also notice that the reflectivity peaks exhibit a strong decrease (increase) in height below (above) ω_L. As can be expected, the reverse behavior occurs for

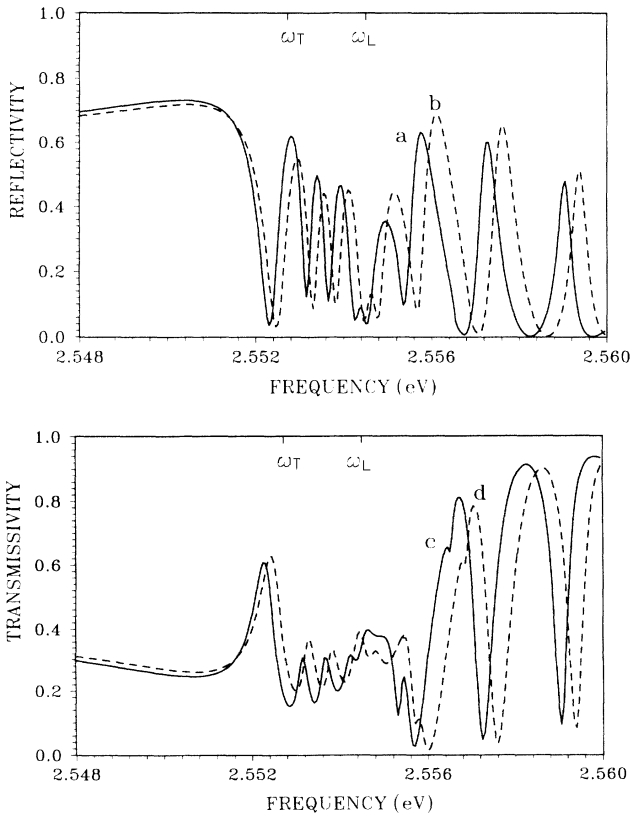

FIG. 2. Normal-incidence reflectivity (above) and transmissivity (below) for a CdS film ($L=1000$ Å) with a repulsive transition layer of thickness a: 60 Å [(a) and (c)] and 90 Å [(b) and (d)]. The height U_S of the surface potential at the surfaces is equal to $U_s=5$ meV.

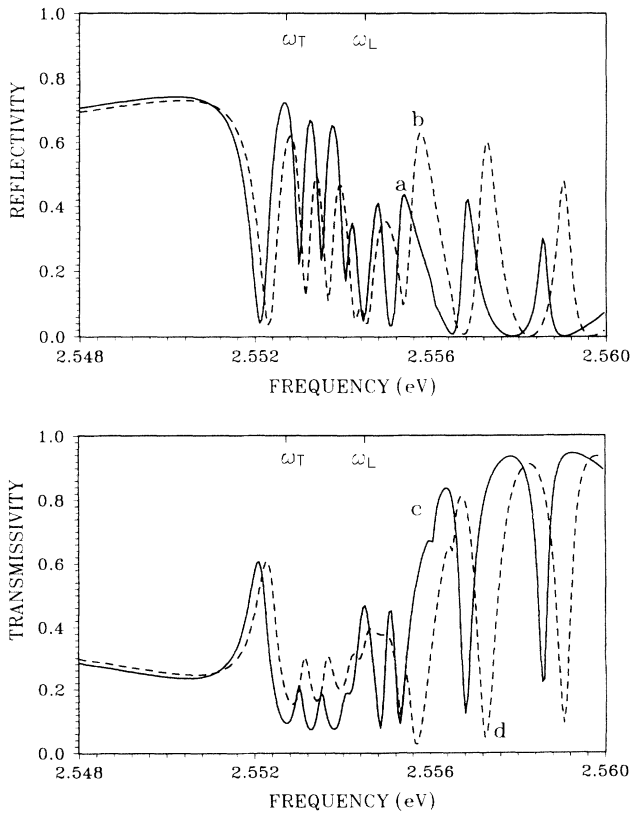

FIG. 3. Normal-incidence reflectivity (above) and transmissivity (below) for a CdS film ($L=1000$ Å) with height U_s of a repulsive surface potential at both surfaces: $U_s=1$ [(a) and (c)] and 5 meV [(b) and (d)]. The thickness a is 60 Å.

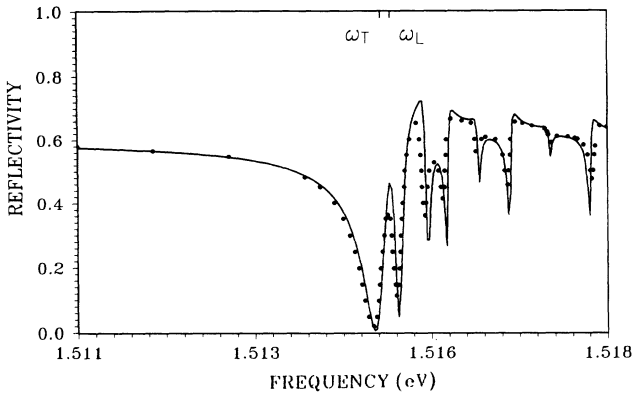

FIG. 4. Normal-incidence reflectivity of a GaAs film ($L=2000$ Å). Solid line is obtained by using the continuous surface potential with $U_s=5$ meV, $a=65$ Å. Dotted curve was taken from Ref. 17: $1/p=65$ Å (see text).

the transmittivity spectra. This effect is often referred to as the "rotation" of the spectrum.

The height U_S of the repulsive exponential potential also affects the positions of the spectral resonances. In Fig. 3 we observe that the resonance frequencies increase as U_S is augmented. A crude estimate of the variation can be obtained from the expression

$$\frac{2a}{\hbar L}(U_s'-U_s)\ . \tag{10}$$

Now let us compare our results with those found from a microscopic model. As mentioned in Sec. I, the microscopic approach[14–20] considers the surface distortion of the exciton wave trough terms as $\exp(-pz)$ and $\exp[-p(L-z)]$, where the parameter $1/p$ represents the transition-layer thickness. To demonstrate the correspondence between the parameter $1/p$ and the quantity a, characterizing the exponential surface potential, we show (Fig. 4) the line shapes of the GaAs reflectance (normal incidence), calculated with our exponential potential and with the microscopic[17] model. The GaAs data utilized are[17] $\hbar\omega_T=1.515$ eV, $\hbar\omega_P=0.07106$ eV, $\varepsilon_0=12.6$, $\hbar\nu=0.035$ meV, and $M=0.298m$ (for the single exciton branch approximation[27]). It is interesting that for equal values of $1/p$ and a, the positions of the resonances could be adjusted with a large value of the potential height (U_s) at the surface.

Although in this section we have principally studied intrinsic-semiconductor films, the results, obtained here, are also valid for samples with repulsive extrinsic contributions in the surface region. In this case, the potential $U(z)$ is no longer symmetric with respect to the center point $z=L/2$.

IV. SURFACE-POTENTIAL WELLS

In this section we shall analyze the optical properties (reflectance and transmission) of thin semiconductor films with near-surface potential wells formed by a surface treatment (see Sec. I and Ref. 21). Let us assume that in the vicinity of the surface $z=0$ [Fig. 1(b)] there is an extrinsic potential valley with depth $|U_m|$ and width Δ. Under condition (6), the parameters U_1, U_2, and a of $U(z)$ (4) are related to U_m and U_0 [$U_0\equiv U(0)$] and Δ by Eq. (I.33). The surface increment of damping $\Delta\nu(z)$ in the extrinsic transition layer will be described by the function (I.34). Considering that the other transition layer (near surface $z=L$) has an intrinsic character (see Sec. III), we can choose

$$U_3=U_{\rm SL}\ ,\quad U_4=0\ , \tag{11}$$

where $U_{\rm SL}$ is the height of $U(z)$ (4) at the surface $z=L$ [$U_{\rm SL}\equiv U(L)$]. Note the effective thickness of the extrinsic transition layer at the left surface is Δ. That of the intrinsic layer at the right surface is b.

Figures 5 and 6 show reflectance and transmission line shapes calculated for a CdS film ($L=1000$ Å). The increase of both width Δ (Fig. 5) and depth $|U_m|$ (Fig. 6) gives rise to a redshift of the spectral resonances. The shift due to the width increase of the potential valley can be estimated by the expression

$$\frac{U_0|\Delta'-\Delta|}{4\hbar L}\ . \tag{12}$$

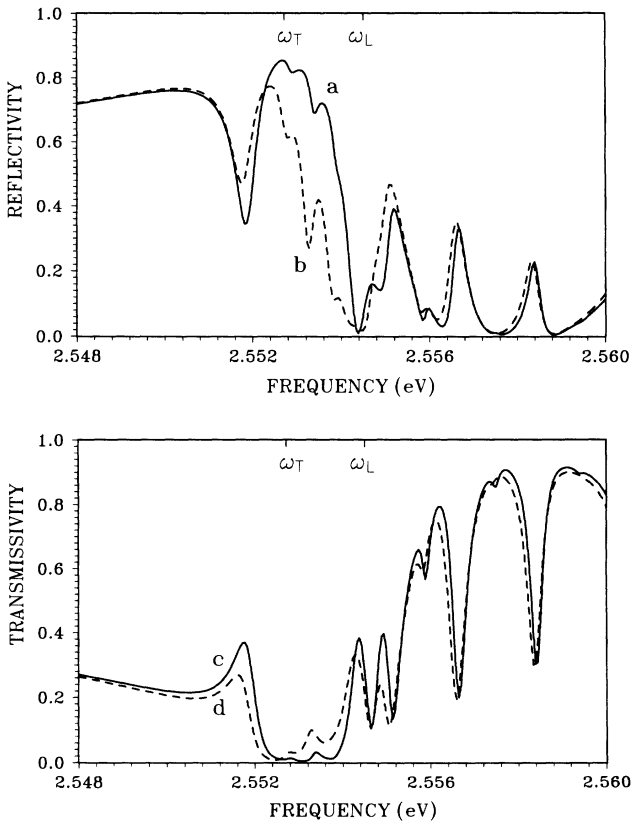

FIG. 5. Normal-incidence reflectivity (above) and transmissivity (below) for a CdS film ($L=1000$ Å) for two widths Δ of the surface-potential well: (a) and (c), $\Delta=130$ Å; (b) and (d), $\Delta=200$ Å. Other parameters of the surface potential used are $U_0=6$ meV, $U_m=-1.5$ meV, $\hbar\Delta\nu_0=0.62$ meV, $U_{\rm SL}=2$ meV, and $b=60$ Å.

We emphasize that this redshift, obtained by increasing the width of the extrinsic potential well, is contrary to the blueshift which arises from increasing the width of a repulsive layer (Sec. III). In principle this result can lead to information about the nature of the surface layer. On the other hand, if $|U_m|$ is increased, then the shift is of the order of the quantity

$$\frac{\Delta}{\hbar L}(U_0)^{1/2}\|U_m'|^{1/2}-|U_m|^{1/2}| \ . \tag{13}$$

The increases of Δ and $|U_m|$ lead to other effects which are similar to those observed in the reflectance of a semiconductor surface.[21] Such effects are the "rotation" of spectral contours with increasing Δ (Fig. 5), and the enhancement near ω_T of the reflectivity (and decrease of the transmission in a thin film) as the well depth $|U_m|$ is augmented (Fig. 6).

When the depth $|U_m|$ is sufficiently large, excitonic bound states appear within the potential well. We shall study the effect of these eigenstates on the optical spectra of thin semiconductor films. We shall use the surface potential $U(z)$ (4) with the following parameters:

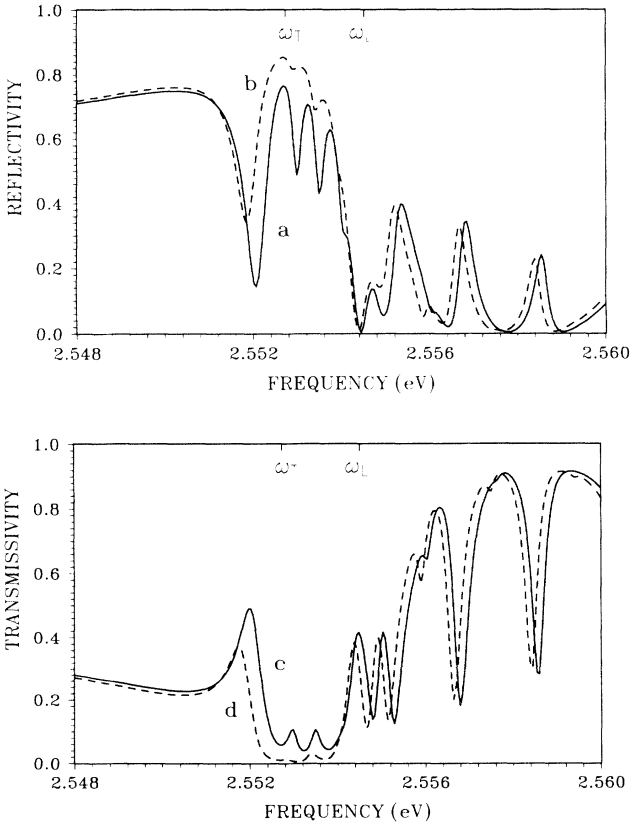

FIG. 6. Normal-incidence reflectivity (above) and transmissivity (below) for a CdS film ($L=1000$ Å) with surface-potential parameters: $\Delta=130$ Å, $U_0=6$ meV, $\hbar\Delta v_0=0.62$ meV, $U_{SL}=2$ meV, and $b=60$ Å; (a) and (c), $U_m=-0.5$ meV; (b) and (d), $U_m=-1.5$ meV.

$$U_1=-2|U_m|e^{z_m/a} \ , \quad U_2=|U_m|e^{2z_m/a} \ ,$$
$$U_3=U_{SL} \ , \quad U_4=0 \ . \tag{14}$$

The chosen potential $U(z)$ (14) is formed by a Morse surface potential, truncated at the surface $z=0$, and by an exponential potential describing the intrinsic transition layer and truncated at the surface $z=L$. Note from condition (6) that it follows that the value of z_m in (14) coincides with the position of the potential-well minimum $[U_m\approx U(z_m), z_m>0]$.

The eigenvalues of the energy, corresponding to the mechanical exciton bound states, are obtained by employing the Schrödinger equation (I.36) for the exciton center-of-mass motion. The boundary conditions for the exciton wave function $\Psi(z)$ have the form

$$\Psi(0)=0 \ , \quad \Psi(L)=0 \ . \tag{15}$$

The solutions of Eq. (I.36) can be written as

$$\Psi(z)=\sum_{l=1}^{2} C_l e^{-v_l z}\left[\sum_{n=0}^{\infty} a_{nl}e^{-nz/a} + \sum_{n=1}^{\infty} b_{nl}e^{-n(L-z)/b}\right] , \tag{16}$$

where C_l ($l=1$ and 2) are constants, and

$$v_1=\left[\frac{2M(\omega_T-\omega)}{\hbar}\right]^{1/2} \ , \quad v_2=-v_1 \ . \tag{17}$$

Within the approximation of noninteracting surfaces [Eq. (6)], the coefficients a_{nl} and b_{nl} in Eq. (16) satisfy the recursion relations

$$a_{n+1,l}=v_m^2\frac{e^{2z_m/a}a_{n-1,l}-2e^{z_m/a}a_{n,l}}{(n+1)(n+1+2v_l a)} \ ,$$
$$b_{n+1,l}=\frac{u^2 b_{n,l}}{(n+1)(n+1-2v_l b)} \tag{18}$$

for $n\geq 1$, and with

$$a_{0,l}=1 \ , \quad a_{1,l}=-v_m^2\frac{2e^{z_m/a}a_{0,l}}{1+2v_l a} \ ,$$
$$b_{1,l}=\frac{u^2 a_{0,l}}{1-2v_l b} \ . \tag{19}$$

In formulas (18) and (19), we introduced the quantities

$$v_m=\frac{a}{\hbar}[2M|U_m|]^{1/2} \ , \quad u=\frac{b}{\hbar}[2MU_{SL}]^{1/2} \ . \tag{20}$$

The excitonic eigenenergies $\hbar\omega_n$ ($\hbar\omega_T-|U_m|<\hbar\omega_n<\hbar\omega_T, n=1,2,\ldots$) are found from the solution of the homogeneous system of algebraic equations (15) for C_l ($l=1$ and 2). The calculation of $\hbar\omega_n$ is carried out numerically. However, for large values of the parameter $U_0=U(0)$ the eigenfrequencies ω_n can be obtained approximately by using the same formula as in the case of a (nontruncated) Morse potential:[28]

$$\omega_n=\omega_T-\frac{|U_m|}{\hbar}\left[1-\frac{1}{v_m}(n-1/2)\right]^2, \qquad (21)$$

with $n<v_m+\frac{1}{2}$.

In Fig. 7 we present results of calculating the normal-incidence reflectivity for CdS films with one (curve *b*) and two (curve *c*) excitonic bound states in the surface-potential well. In Fig. 7 (curve *a*) a characteristic spectrum of a film without near-surface localized excitons is also included for comparison. The results show a considerable enhancement of the reflectivity near eigenfrequencies ω_n. Thus the excitonic bound states are manifested in the spectrum as broad peaks, which smooth the resonances for $\omega\leq\omega_T$. Clearly, the resonances associated with the near-surface-potential well predominate over the Fabry-Perot resonances related to the thin film as a whole. It is noteworthy that this fading of spectral resonances in films with treated surfaces has also been obtained by using right-angled potential wells.[24] With increasing potential well depth $|U_m|$, the eigenfrequencies and corresponding broad peaks are shifted to lower frequencies; see line ω_1. According to Eq. (21), their shift is given by

$$\omega_n(U_m')-\omega_n(U_m)=-\frac{|U_m'|-|U_m|}{\hbar}+\left[\frac{2}{M}\right]^{1/2}\frac{n-1/2}{a}(|U_m'|^{1/2}-|U_m|^{1/2}). \qquad (22)$$

Note (Fig. 7) that the shift of the first broad peak ($n=1$) is larger than the shift of the Fabry-Perot spectral resonances.

The appearance of near-surface-localized excitons also affects the behavior of the polarization $P(z)$. We computed the field $|P(z)|$ (Fig. 8) at the frequencies $\omega_{m1}=2.5516$ eV and $\omega_{m2}=2.55305$ eV of the broad peaks in Fig. 7(c). The frequencies ω_{m1} and ω_{m2} do not coincide exactly with $\omega_1=2.55138$ eV and $\omega_2=2.55271$ eV because of polariton effects.[21] Within the potential well, $|P(z)|$ has one and two sharp maxima for the first and the second exciton eigenstates, respectively. These maxima are associated with the extrema of the wave functions $\Psi_n(z)$ ($n=1$ and 2) of the localized excitons. Far from the treated surface the field $|P(z)|$ undergoes oscillations. They are due to the modes $s=1$ and 3 in Eq. (5), which have real wave-vector components q_1 and q_3 ($q_3=-q_1$) at frequencies ω_{m1} and ω_{m2} ($\omega_{m2}<\omega_L$). Thus the period of the oscillations of $|P(z)|$ in Fig. 8 is given by π/q_1.

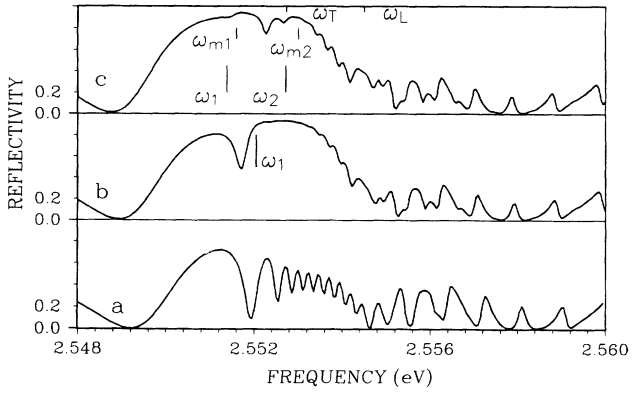

FIG. 7. Normal-incidence reflectivity for a CdS film ($L=2000$ Å). Curve *a* corresponds to an intrinsic surface potential $U_S=2$ meV, $a=60$ Å. Curves *b* and *c* were calculated for extrinsic surface-potential wells with one and two excitonic bound states, respectively ($z_m=60$ Å, $a=60$ Å, $\Delta v_0=0$, $U_{SL}=2$ meV, $b=60$ Å; *b*, $U_m=-2$ meV; *c*, $U_m=-3$ meV).

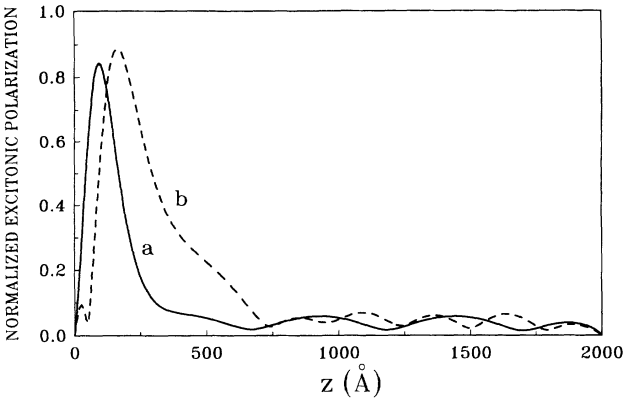

FIG. 8. Graphs of the absolute value of the excitonic polarization $|P(z)/E_i|$ at the frequencies $\omega_{m1}=2.5516$ eV (a), $\omega_{m2}=2.55305$ eV (b), and with the parameters of the surface potential as in Fig. 7 (c).

Until now, we have considered only one treated surface in the film. When both transition layers of a thin semiconductor film are extrinsic, its optical spectra may have a complicated structure of broad peaks and resonances. Nevertheless, in such a situation our model can also be applied to interpret experimental spectra by adjusting the remaining parameter U_4 in Eq. (4).

V. CONCLUSION

The model proposed here for the surface potential of a thin semiconductor film allows us to associate features of optical spectra with the nature of the near-surface transition layer of the sample. From the shift of spectra resonances one can obtain information about the extrinsic contribution to the surface potential. This model is especially useful for studying the generation of excitonic bound states within an extrinsic potential well, and their influence on optical spectra. The localization of excitons near a treated surface manifests itself in the reflectivity for *s*-polarized light as broad peaks (and in the transmissivity as minima) which smooth the spectral resonances. The high sensitivity of the optical spectra of thin semiconductor films to the surface structure may be utilized for diagnosing the state of the near-surface transition layer.

ACKNOWLEDGMENT

This work was partially supported by the Consejo Nacional de Ciencia y Tecnología (CONACyT) under Grant No. 2048 E 9302.

APPENDIX: CALCULATION OF a_{ns} AND b_{ns}

Substituting the excitonic polarization $P(z)$ (5) into Eq. (3), we obtain an equation for the coefficients a_{ns} and b_{ns} ($s=1$, 2, 3, and 4):

$$
\begin{aligned}
&\sum_{n=1}^{\infty}\left\{[n^4-4in^3q_sa]\frac{a_{ns}}{a^4}e^{-nz/a}+[n^4+4in^3q_sb]\frac{b_{ns}}{b^4}e^{-n(L-z)/b}\right.\\
&\quad+n^2\left[\frac{a_{ns}}{a^2}e^{-nz/a}+\frac{b_{ns}}{b^2}e^{-n(L-z)/b}\right][\alpha_1-\alpha_0U_1e^{-z/a}-\alpha_0U_2e^{-2z/a}-\alpha_0U_3e^{-(L-z)/b}-\alpha_0U_4e^{-2(L-z)/b}]\\
&\quad+n\left[-\frac{a_{ns}}{a}e^{-nz/a}+\frac{b_{ns}}{b}e^{-n(L-z)/b}\right]\\
&\quad\times\left[\alpha_2-\frac{2\alpha_0U_1}{a}(iq_sa-1)e^{-z/a}-\frac{2\alpha_0U_2}{a}(iq_sa-2)e^{-2z/a}\right.\\
&\qquad-\frac{2\alpha_0U_3}{b}(iq_sb+1)e^{-(L-z)/b}\\
&\qquad\left.\left.-\frac{2\alpha_0U_4}{b}(iq_sb+2)e^{-2(L-z)/b}\right]\right\}\\
&-\left[\sum_{n=0}^{\infty}a_{ns}e^{-nz/a}+\sum_{n=1}^{\infty}b_{ns}e^{-n(L-z)/b}\right]\\
&\quad\times\left[\frac{\alpha_0U_1}{a^2}(1-2iq_sa+\alpha_3a^2)e^{-z/a}+\frac{\alpha_0U_2}{a^2}(4-4iq_sa+\alpha_3a^2)e^{-2z/a}\right.\\
&\qquad\left.+\frac{\alpha_0U_3}{b^2}(1+2iq_sb+\alpha_3b^2)e^{-(L-z)/b}+\frac{\alpha_0U_4}{b^2}(4+4iq_sb+\alpha_3b^2)e^{-2(L-z)/a}\right]=0\ .
\end{aligned}
\tag{A1}
$$

Here we have introduced the following notation:

$$
\begin{aligned}
&\alpha_0=\frac{2M}{\hbar^2}\ ,\quad \alpha_1=-6q_s^2+\Gamma_B^2+\varepsilon_0\frac{\omega^2}{c^2}-q_x^2\ ,\\
&\alpha_2=-4iq_s^3+2iq_s\left[\Gamma_B^2+\varepsilon_0\frac{\omega^2}{c^2}-q_x^2\right]\ ,\\
&\alpha_3=-q_s^2+\varepsilon_0\frac{\omega^2}{c^2}-q_x^2\ .
\end{aligned}
\tag{A2}
$$

The quantity Γ_B^2 is defined by Eq. (I.7). We solved Eq. (A1) by supposing that the inequalities (6) are satisfied. Thus terms having functions, which are exponentially small in the whole interval $0\le z\le L$, were neglected. These functions are

$$
e^{-z/a}e^{-n(L-z)/b}\ ,\quad e^{-2z/a}e^{-n(L-z)/b}\ ,\quad e^{-(L-z)/b}e^{-nz/a}\ ,\quad e^{-2(L-z)/b}e^{-nz/a}\ ,
$$

with $n\ge 1$. After this simplification, from Eq. (A1) we obtain the recursion relations for a_{ns} and b_{ns} ($s=1$, 2, 3, and 4) for $n\ge 2$:

$$
\begin{aligned}
a_{ns}&=\frac{2Ma^2[(\kappa-n)^2+\beta a^2][U_2a_{n-2,s}+U_1a_{n-1,s}]}{\hbar^2[n^4-4\kappa n^3+[6\kappa^2+(\Gamma_B^2+\beta)a^2]n^2-[4\kappa^3+2\kappa(\Gamma_B^2+\beta)a^2]n]}\ ,\\
b_{ns}&=\frac{2Mb^2[(\lambda+n)^2+\beta b^2][U_4b_{n-2,s}+U_3b_{n-1,s}]}{\hbar^2[n^4+4\lambda n^3+[6\lambda^2+(\Gamma_B^2+\beta)b^2]n^2+[4\lambda^3+2\lambda(\Gamma_B^2+\beta)b^2]n]}\ ,
\end{aligned}
\tag{A3}
$$

where κ and λ are defined by $\kappa=iq_sa$ and $\lambda=iq_sb$ ($s=1$, 2, 3, and 4), respectively. The first terms of each relation are

given by the expressions

$$a_{1s}=\frac{2Ma^2[(\kappa-1)^2+\beta a^2]U_1 a_{0s}}{\hbar^2[1-4\kappa+6\kappa^2+(\Gamma_B^2+\beta)a^2-4\kappa^3-2\kappa(\Gamma_B^2+\beta)a^2]}\,,$$
$$b_{1s}=\frac{2Mb^2[(\lambda+1)^2+\beta b^2]U_3 a_{0s}}{\hbar^2[1+4\lambda+6\lambda^2+(\Gamma_B^2+\beta)b^2+4\lambda^3+2\lambda(\Gamma_B^2+\beta)b^2]}\,, \tag{A4}$$

and $a_{0s}=1$.

[1] *Excitons in Confined Systems,* edited by R. Del Sole, A. D'Andrea, and A. Lapiccirella, Springer Proceedings in Physics Vol. 25 (Springer, Berlin, 1988).

[2] V. A. Kiselev, I. V. Makarenko, B. S. Razbirin, and I. N. Ural'tsev, Fiz. Tverd. Tela (Leningrad) **19**, 2348 (1977) [Sov. Phys. Solid State **19**, 1374 (1977)].

[3] P. Halevi, in *Spatial Dispersion in Solids and Plasmas,* edited by P. Halevi (Elsevier, Amsterdam, 1992), Chap. 6.

[4] M. F. Bishop, Solid State Commun. **20**, 779 (1976).

[5] D. L. Johnson, Phys. Rev. B **18**, 1942 (1978).

[6] P. Halevi, G. Hernández-Cocoletzi, and J. A. Gaspar-Armenta, Thin Solid Films **89**, 271 (1982).

[7] J. A. Gaspar-Armenta and P. Halevi, Rev. Mex. Fis. **33**, 599 (1988).

[8] P. Halevi, in *Excitons in Confined Systems* (Ref. 1), p. 2.

[9] J. J. Hopfield and D. G. Thomas, Phys. Rev. **132**, 563 (1963).

[10] V. A. Kiselev, B. S. Razbirin, and I. N. Uraltsev, Phys. Status Solidi B **72**, 161 (1975).

[11] I. V. Makarenko, I. N. Uraltsev, and V. A. Kiselev, Phys. Status Solidi B **98**, 773 (1980).

[12] V. A. Kiselev, I. N. Uraltsev, and I. V. Makarenko, Solid State Commun. **53**, 591 (1985).

[13] T. Mita and N. Nagasawa, Solid State Commun. **44**, 1003 (1982).

[14] K. Cho and M. Kawata, J. Phys. Soc. Jpn. **54**, 4431 (1985).

[15] K. Cho and H. Ishihara, in *Excitons in Confined Systems* (Ref. 1), p. 90.

[16] A. D'Andrea, R. Del Sole, and K. Cho, Europhys. Lett. **11**, 169 (1990).

[17] K. Cho and H. Ishihara, J. Phys. Soc. Jpn. **59**, 754 (1990).

[18] K. Cho, A. D'Andrea, R. Del Sole, and H. Ishihara, J. Phys. Soc. Jpn. **59**, 1853 (1990).

[19] A. D'Andrea and R. Del Sole, Phys. Rev. B **41**, 1413 (1990).

[20] H. Ishihara and K. Cho, Phys. Rev. B **41**, 1424 (1990).

[21] F. Pérez-Rodríguez and P. Halevi, Phys. Rev. B **45**, 11 854 (1992).

[22] P. Halevi and F. Pérez-Rodríguez, Fiz. Nizk. Temp. **18**, 1135 (1992) [Sov. J. Low Temp. Phys. **18**, 795 (1992)].

[23] F. Pérez-Rodríguez and P. Halevi, Phys. Rev. B **48**, 2016 (1993).

[24] V. A. Kiselev, Solid State Commun. **43**, 471 (1982).

[25] V. A. Kiselev, Fiz. Tverd. Tela (Leningrad) **20**, 1191 (1978) [Sov. Phys. Solid State **20**, 685 (1978)].

[26] Peter Y. Yu and F. Evangelisti, Phys. Rev. Lett. **24**, 1642 (1979).

[27] A. D'Andrea and R. Del Sole, Phys. Rev. B **25**, 3714 (1982).

[28] L. D. Landau and E. M. Lifshitz, *Quantum Mechanics Non-Relativistic Theory* (Addison-Wesley, Reading, MA, 1977).